Journal of Power Sources 196 (2011) 10120–10125

Contents lists available at ScienceDirect

Journal of Power Sources

journal homepage: www.elsevier.com/locate/jpowsour

Electrochemical stability of lithium bis(oxatlato) borate containing solid polymer electrolyte for lithium ion batteries

Ding Zhang[a], Hui Yan[a], Zhi Zhu[a], Huan Zhang[b], Jian Wang[a], Qilu[a,*]

[a] Beijing National Laboratory for Molecular Sciences, Institute of Applied Chemistry, College of Chemistry and Molecular Engineering, Peking University, Beijing 100871, PR China
[b] 2 CITIC GUOAN MGL Company, Beijing 102200, PR China

ARTICLE INFO

Article history:
Received 5 July 2011
Accepted 15 July 2011
Available online 22 July 2011

Keywords:
Solid polymer electrolyte
Electrochemical stability
Poly(ethylene oxide)
Lithium bis(oxatlato) borate
Magnesium oxide

ABSTRACT

The electrochemical stability of lithium bis(oxatlato) borate (LiBOB) containing solid polymer electrolyte has been evaluated both by inert electrode and real cathodes. Enhanced intrinsic anodic stability and decreased interface impedance, are obtained by addition of nano-sized MgO to PEO_{20}–LiBOB. It is also found that the LiBOB-containing SPEs exhibit prominent kinetic stability between 3.0 and 4.5 V. For cells using SPEs as the separators, good cycling performance is obtained for real 4 V class cathodes material $LiNi_{1/3}Co_{1/3}Mn_{1/3}O_2$ and $LiCoO_2$. The Li|PEO_{20}–LiBOB|$LiNi_{1/3}Co_{1/3}Mn_{1/3}O_2$ cell takes an initial capacity of 156.8 mAh g^{-1}, with retention of 142.5 mAh g^{-1} after 20 cycles at 0.2*C*-rate. The cell also works well up to 1*C*-rate. The addition of nano-sized MgO into PEO_{20}–LiBOB readily reduces the irreversible capacity per cycle, both for $LiNi_{1/3}Co_{1/3}Mn_{1/3}O_2$ and $LiCoO_2$ cathodes. In addition, the critical role of LiBOB in obtaining kinetic stability and passivating ability towards cathodes are specially discussed.

1. Introduction

Currently general electrolytes for lithium ion secondary batteries mainly relate to nonaqueous electrolytes. They are typically lithium salts solvated by mixture of cyclic carbonates and linear carbonates [1–5]. For example, $LiPF_6$ (lithium hexafluorophosphate) works as solute in the mixture of EC and DMC (ethylene carbonates and dimethyl carbonate).

Comparatively, solid polymer electrolytes (SPEs) are using thermal stable and environmental friendly polymers as the solvents. Among various SPEs, PEO–LiX (X = ClO_4^-, $SO_3CF_3^-$ and so on) systems have received the most extensive attention. Their major disadvantages [6,7] are the poor ionic conductivity (10^{-8} to 10^{-6} S cm^{-1}) at ambient temperature and the low cation transference numbers (about 0.3). However, the good thermal stability, qualified compatibility towards lithium metal anode and the flexibility to volume change of electrodes still enable them promising components for lithium ion secondary batteries.

Nano-sized material Al_2O_3 and TiO_2 powders have been introduced to PEO–LiX systems [6], thereby improving ionic conductivities at ambient temperatures. Addition of nano-materials also resulted in improved cation transference number [8], decreased interface impedance [9,10] and enhanced anodic stability [8] as well as increased mechanical strength. Previous reports have intensively studied the performance of such SPEs with 3 V class cathodes, such as $LiFePO_4$ [11–13], $LiMn_3O_6$ [12] and V_2O_5. Recently there were several reports about the compatibility between polymer–lithium salt complexes and 4 V class cathodes, such as $LiCoO_2$ and $LiMn_2O_4$. Poly(ethylene oxide-co-propylene oxide) [14] was applied in $LiCoO_2$ cells with LiTFSI (lithium bis(trifluoromethanesulfonyl)imide, or LiIm) as the lithium salt. The upper voltage limit was set at 4.1 V. Watanabe and co-authors [15] investigated the performance of cells between 3.0 and 4.2 V by using SPE P(EO/MEEGE)–LiTFSI as the separator and $LiCoO_2$ as the cathode. In these reports modified polymers and high performance LiTFSI are adopted to obtain improved anodic stability for the electrolyte. The lithium salt, in principle, not only provides charge carriers but also participates in redox process occurring at the surfaces of electrodes [16,17]. Thus it can be a key factor in determining actual electrochemical stability of electrolyte. LiBOB is electrochemically stable up to 4.5 V [18], with capability to passivate an Al current-collector up to 6.0 V [19]. Besides its extraordinary capability to passivate graphite in neat propylene carbonate [20], the salt also provides thermal stability up to about 300 °C and low manufacturing cost [21].

If PEO–LiBOB complex can support the operation of 4 V class cathodes, it will be rather economical. We consider adopting LiBOB and nano-material to obtain improved performance for traditional PEO-based SPEs. Scrosati et al. [22] reported their investigation on the fundamental structural behavior and electrochemical properties of PEO–LiBOB electrolytes. They exhibit ionic conductivities about 10^{-5} S cm^{-1} at room temperature and near 10^{-3} S cm^{-1}

* Corresponding author. Tel.: +86 010 627 538 68; fax: +86 010 627 552 90.
E-mail address: qilu@pku.edu.cn (Qilu).

0378-7753/$ – see front matter © 2011 Elsevier B.V. All rights reserved.
doi:10.1016/j.jpowsour.2011.07.056

above 60 °C. And their cation transference number varies between 0.25 and 0.30.

In this work the electrochemical stability of PEO–LiBOB type SPEs both will be investigated. To date, the electrochemical stability of such SPEs has not been examined, especially towards 4 V class cathodes. It shows that adequate stability is obtained on supporting reversible operation of the most widely applied cathodes including $LiCoO_2$ and $LiNi_{1/3}Co_{1/3}Mn_{1/3}O_2$. The reason that LiBOB-containing SPEs present adequate electrochemical stability towards the two cathodes is analyzed in detail.

2. Experimental

2.1. Chemical reagents

PEO (M_w 600000; AR grade) was purchased from Sigma–Aldrich. The lithium salt, LiBOB, 98% purity, was kindly donated by Chemetall Inc. Lithium perchlorate ($LiClO_4$, AR, 99% purity) and acetonitrile (AR, 99.5% purity) were both purchased from Beijing Reagent Co., Ltd. All reagents were used without further purification. Cathode material $LiNi_{1/3}Co_{1/3}Mn_{1/3}O_2$ was synthesized in our lab according to the literature procedure [23]. Cathode material $LiCoO_2$ was prepared by evenly grinding the mixture of Li_2CO_3 and Co_3O_4 (molar ration, Li:Co = 1.05) and heating the mixture at 600 °C for 5 h and later at 900 °C for 5 h. Nano-size magnesium oxide (MgO) was obtained from Sigma–Aldrich with an average diameter of 40 nm.

2.2. Preparation of the PEO_{20}–LiBOB electrolyte membranes

The solid polymer electrolyte membranes were prepared by classic solvent casting technique. The molar ratio of PEO to lithium salt was fixed at 20. Before the preparation of SPE, lithium salts were thoroughly dried in vacuum box at 130 °C for 24 h. Specific amounts of PEO powder and lithium salt were mixed in acetonitrile. For preparing composite SPE, 5 wt% nano-sized MgO, relative to the summed mass of PEO and lithium salt, is also added to the mixture. The mixture was vigorously stirred for 48 h to reach good homogeneity in seal condition and then the solvent was partly evaporated by heating the mixture under continuing stir. The concentrated mixture was cast onto home made dish-like Teflon molds and dried under slow anhydrous nitrogen flow. Some self-standing 100 μm thick transparent membranes were obtained. When MgO is added, the prepared membranes turn white and opaque but hardly change in strength. In this work, three SPEs are prepared, including PEO_{20}–LiBOB, PEO_{20}–LiBOB–5 wt% MgO and PEO_{20}–$LiClO_4$.

2.3. Electrochemical measurements

The prepared SPE membranes were shaped into round sheets after drying at 50 °C for 2 days under vacuum and assembled into experimental R2032 cells in an argon-filled glove box (Braun, Germany; working condition, H_2O: 3 ppm, O_2: 1 ppm). The configuration of cell for CV measurements was SS (stainless steel)|SPE|Li (lithium metal), with SS as the working electrode and lithium metal sheet as the counter electrode and the reference electrode. Cyclic-voltammetry (CV) measurements were performed from the OCVs of the cells over a sweep rate of 5 mV s^{-1} at various temperatures. Voltage ranges for each test were changed depending on the purpose.

Symmetric cell Li|SPE|Li (lithium metal) was also fabricated and kept constantly at 80 °C in hot box and the evolution of interface impedance is recorded by measuring its electrochemical impedance spectra (EIS) after different periods. EIS measurements were recorded at the open-circuit voltages (OCV) in the frequency range of 0.01 Hz to 100 kHz, with a 5 mV excitation signal.

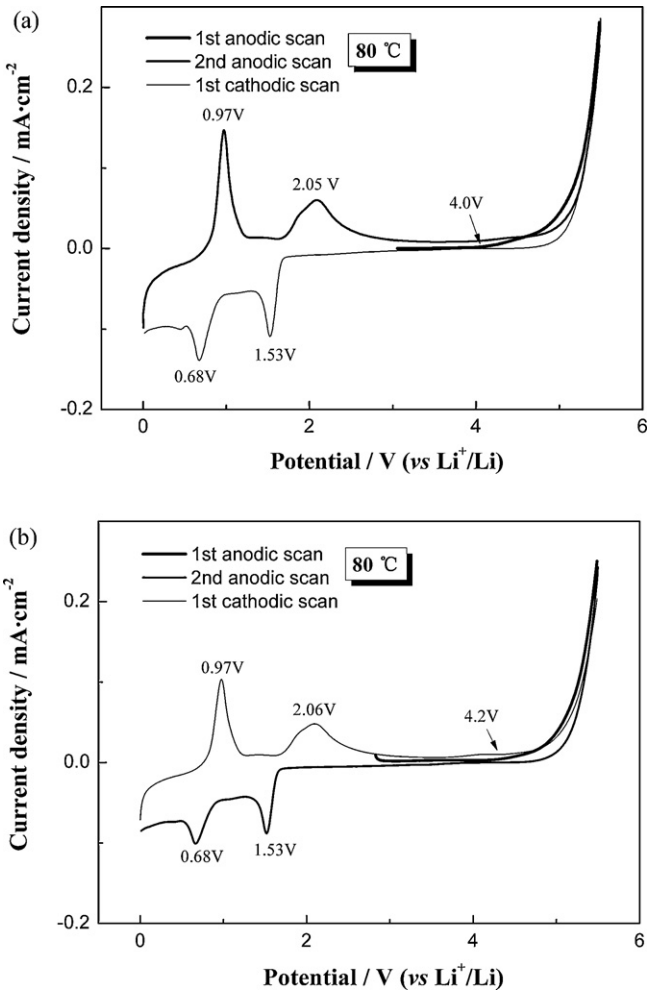

Fig. 1. CV curves of PEO_{20}–LiBOB (a) and PEO_{20}–LiBOB–5 wt% MgO (b) at 80 °C. The first anodic scan, first cathodic scan and second anodic scan are measured in the voltage range of 0–5.5 V.

A surface morphology (SEM) study of the prepared cathodes active material was performed using a JEOL JSM-5600LV electron microscope. The XRD measurements were carried out using a Rigaku MultiFlex diffractometer, equipped with a monochromator and a Cu target tube. A continuous scan mode over a 2θ range of 10–90° with a step size of 0.02° and scan rate of 4.0° min^{-1} was adopted.

The charge–discharge tests were performed on coin type cell (R2032). A composite cathode was prepared by evenly mixing $LiNi_{1/3}Co_{1/3}Mn_{1/3}O_2$ or $LiCoO_2$ (70 wt%) with conductive graphite (15 wt%, TIMREX Inc., KS-15), PEO_{20}–LiBOB (15 wt%) in acetonitrile and then spreading the mixture onto clean aluminum foil. Active material load is about 10 mg cm^{-2}. Cells were fabricated in the argon-filled glove box, using round Li metal sheets as counter electrodes and prepared SPEs as the separators. The cells were galvanostatically cycled on a Land CT2001A battery Cycler (Wuhan Jinnuo Electronics Co., Ltd., China) at 80 °C.

3. Results and discussion

The electrochemical stability of PEO_{20}–LiBOB–5 wt% MgO, as well as that of PEO_{20}–LiBOB, is measured by employing cyclic voltammetry (Fig. 1). The addition of nano-MgO enables PEO_{20}–LiBOB to decompose at more positive voltage, indicating an improved anodic stability. Actually there lacks a consistent quantitative criterion for judging whether or not an electrolyte

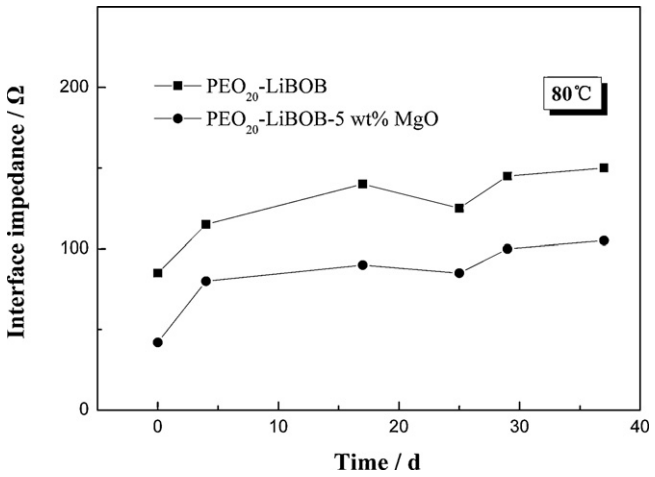

Fig. 2. Time evolution of interface impedance between a lithium metal electrode and the prepared SPEs PEO_{20}–LiBOB and PEO_{20}–LiBOB–5 wt% MgO at 80 °C. Data is obtained by fitting the corresponding semicircle in electrochemical impedance spectra with Zview software.

begins oxidative decomposition above a certain voltage. Handa et al. [24] suggested an exchange current density of 0.03 mA cm^{-2} as the indicator of electrolytes oxidative decomposition by studying several liquid nonaqueous electrolytes on different solvents. Due to the faster CV scan speed adopted, tighter current density of 0.003 mA cm^{-2} is used to estimate the oxidization onset voltage in this work.

As shown in Fig. 1a, the current density is approximate 0.003 mA cm^{-2} at 4.0 V and begins to increase obviously from this voltage for the first anodic scan of PEO_{20}–LiBOB. It corresponds to the start of oxidative decomposition of the electrolyte. Violent oxidation is revealed by the exponentially increased current density above 5 V. In the second cathodic scan and second anodic scan, it is seen that two anodic peaks appear separately at 0.97 V and 2.05 V, while two cathodic peaks appear separately at 1.53 V and 0.68 V. The peaks at 0.97 V and 0.68 V are possibly due to reaction closely related to LiBOB, i.e. the reduction and oxidization of ion species formed by dissociation of lithium salt in PEO segments. The surface chemistry on lithium metal anode was found to be dominated by salt anion reduction for organic solvent free polymer electrolytes [25]. The peaks at 1.53 V and 2.05 V are mainly attributed to redox closely related to trace water molecule that exists in the SPE. Experimentally, the peak density is clearly lowered compared to those at 0.97 V and 0.68 V when the SPEs contained less water by preparing the SPEs under high vacuum or in a Ar-filled glove box.

When nano-sized MgO is added, the initial oxidative decomposition is observed at 4.2 V (Fig. 1b), more positive than that of PEO_{20}–LiBOB. The following violent decomposition of electrolyte occurs similarly above 5 V. Observed redox peaks, in the low voltage range of 0–2.5 V, have nearly identical peaks voltages but with typical lower peak densities. It is concluded that the addition of MgO enhances the anodic stability for PEO_{20}–LiBOB system. Redox of electrolyte components in the low voltage range seems to be suppressed, which is indicated by the lowered intensities of redox peaks. Nano-sized MgO can efficiently absorb trace water and unstable compounds in PEO_{20}–LiBOB, and thus favor the electrochemical stability especially the anodic stability.

Symmetric lithium cells, using lithium metal as both electrodes, are used to study the effect of MgO on the interface impedance of PEO_{20}–LiBOB. EIS features of interface impedance of PEO_{20}–LiBOB and PEO_{20}–LiBOB–5 wt% MgO are continually monitored during 37 days and the results are shown in Fig. 2. It is observed that adoption of MgO succeeds in dramatically reducing the interface impedance

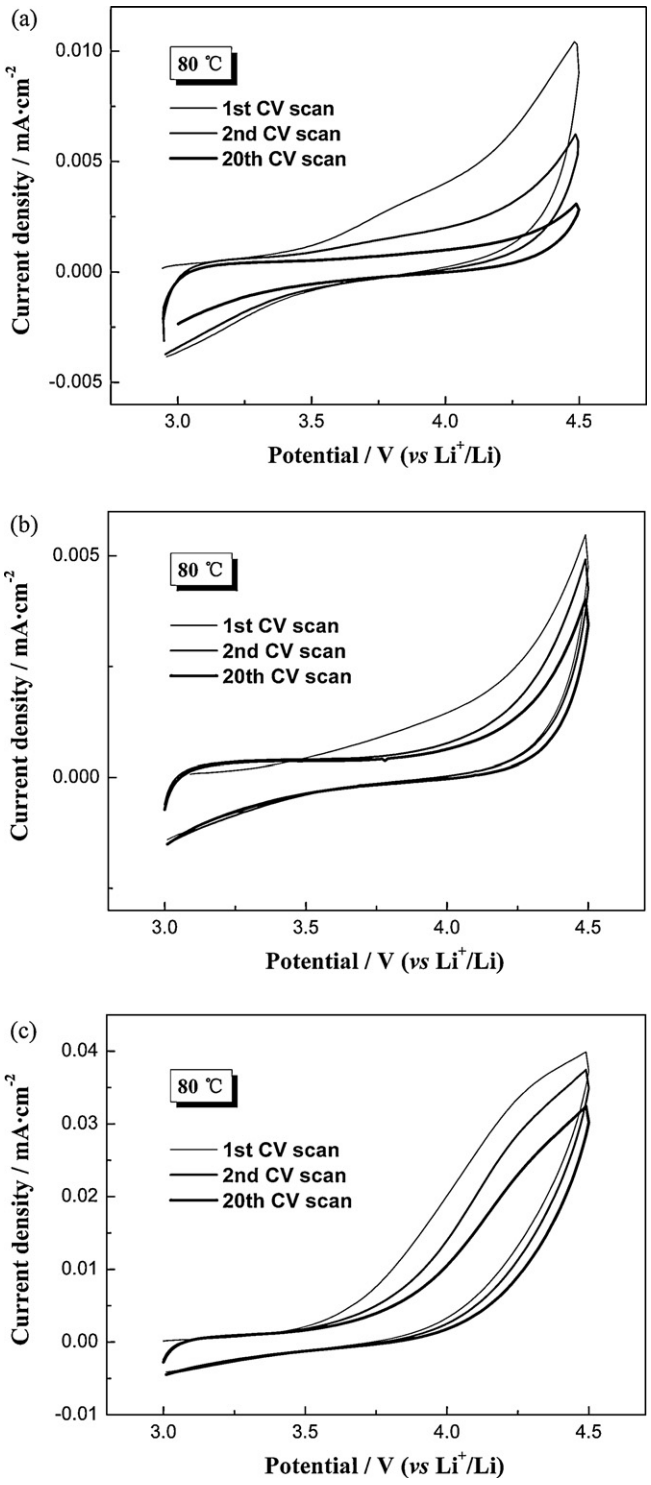

Fig. 3. CV curves of the first, second and twentieth full scan in the voltage range of 3.0–4.5 V for PEO_{20}–LiBOB (a), PEO_{20}–LiBOB–5 wt% MgO (b) and PEO_{20}–$LiClO_4$ (c) at 80 °C.

by about 50% for fresh cells. Furthermore, the decrease is kept over a month as the cells become aged. MgO might suppress the reduction of LiBOB and thus favor lower interface impedance.

Further CV tests, simulating charge–discharge cycles in cells for electrolyte, are performed for PEO_{20}–LiBOB, PEO_{20}–LiBOB–5 wt% MgO and PEO_{20}–$LiClO_4$. The voltage range is set between 3.0 and 4.5 V. Results are presented in Fig. 3. A 'kinetic stability' is observed

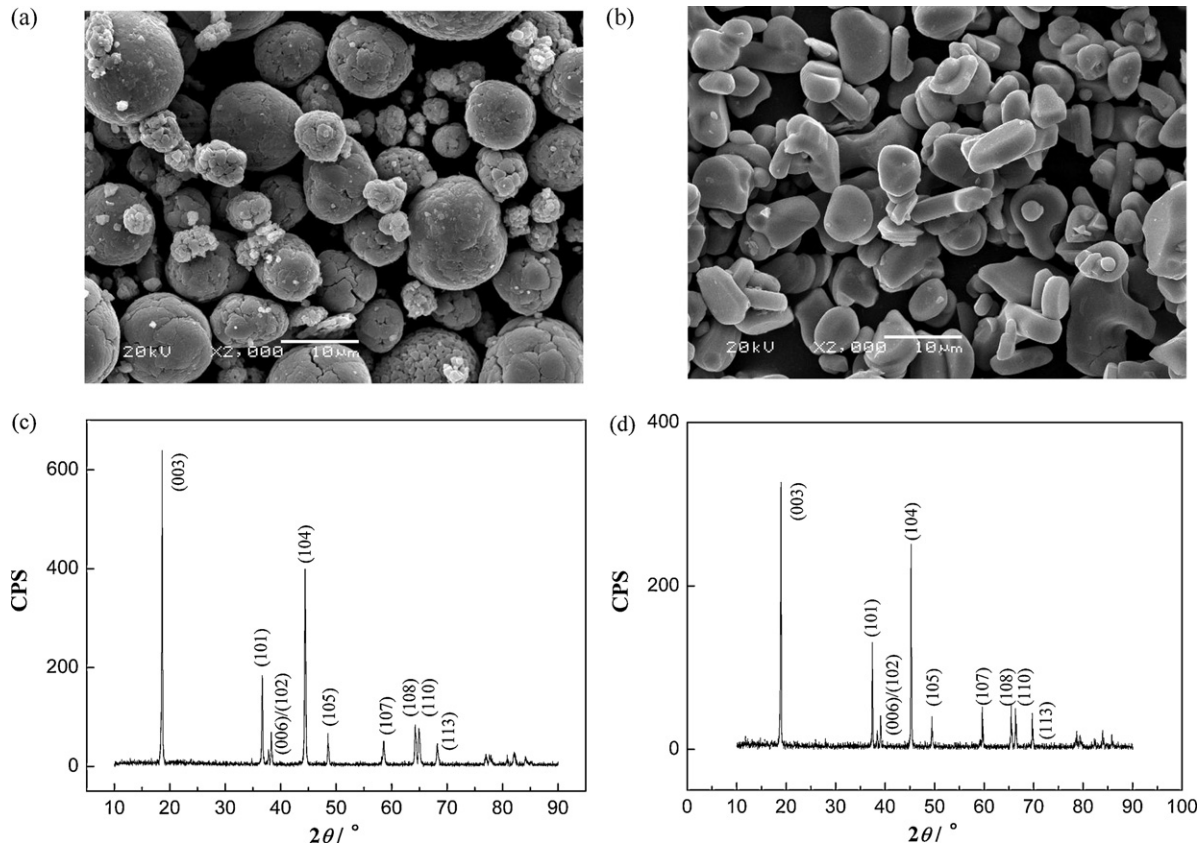

Fig. 4. SEM images of prepared $LiNi_{1/3}Co_{1/3}Mn_{1/3}O_2$ (a) and $LiCoO_2$ (b) and the corresponding XRD pattern (c) and (d).

for PEO_{20}–LiBOB, and the nano-MgO added sample also supports this property.

As to the PEO_{20}–LiBOB sample, a typical anodic current density at 4.5 V reduces from initial 0.01 mA cm^{-2} to 0.003 mA cm^{-2}, while the current density at 3.0 V remains constant around 0.003 mA cm^{-2} during 20 full CV cycles shown in Fig. 3a. The measured initial anodic current density at 4.5 V is much larger than presumed decomposition criterion. However, its significant decrease finally meets the criterion. As to the MgO-added example in Fig. 3b, smaller initial anodic current densities are observed and same tendency of decrease on current density is obtained. The anodic current density at 4.5 V reduces from 0.005 mA cm^{-2} to 0.004 mA cm^{-2} and the cathodic current at 3.0 V remain constant at 0.001 mA cm^{-2} during 20 CV cycles.

Passivation of cathode surfaces, which prevented bulk electrolytes from further decomposition, has been recognized [26]. For the LiBOB containing SPEs, it seems that the oxidization product acts the same way during repeated anodic process. An efficient passivating layer forms even though the cathode here is an inert electrode. The passivation enables the electrolyte to support higher electrode potentials which originally lie outside the electrolyte stability window. Thus a 'kinetic stability' above 4 V is obtained for LiBOB containing SPEs. The kinetic stability for electrolyte is specially discussed in a review literature by Goodenough and Kim [27]. Despite the fact that real anodic stability of electrolytes is often inferior to that measured by inert electrodes, the kinetic stability in 3.0–4.5 V, indicated by the qualified value of current density shown above, might have fulfilled the requirements of 4 V class cathodes.

In contrast, decreased anodic current density, upon CV cycles, has also been observed in PEO_{20}–$LiClO_4$ example shown in Fig. 3c. Anodic current densities at 4.5 V are 0.077 and 0.070 mA cm^{-2}, respectively, for the first and second cycle. When 20 cycles is finished, the anodic current density at 4.5 V is 0.034 mA cm^{-2}. Such anodic current density reveals significant oxidative decomposition of electrolyte for PEO–$LiClO_4$. Thus it will hinder the operation of cathodes above 4 V for $LiClO_4$-containing PEO-based SPEs. The current density at 3.0 V, on the other side, remains constant at 0.004 mA cm^{-2}. It is possibly due to similar reaction activity of PEO–$LiClO_4$ as PEO_{20}–LiBOB near 3.0 V. However, it is clear that LiBOB-containing SPEs have superior overall electrochemical stability over PEO–$LiClO_4$ system.

Two cathodes, $LiNi_{1/3}Co_{1/3}Mn_{1/3}O_2$ and $LiCoO_2$, are adopted to evaluate the practical electrochemical stability of PEO_{20}–LiBOB and PEO_{20}–LiBOB–5 wt% MgO. The surface images and XRD patterns are indicated in Fig. 4. The particle of prepared $LiCoO_2$ appears potato-like, round and irregular with smooth surface. Its average diameter is about 5 μm. The powder of $LiNi_{1/3}Co_{1/3}Mn_{1/3}O_2$ is spherical and each powder is composed of many small dish-shaped particles. Its average diameter is about 10 μm. XRD diagrams of $LiCoO_2$ and $LiNi_{1/3}Co_{1/3}Mn_{1/3}O_2$ both display a typical single-phase α-$NaFeO_2$ layered structure without impurity phase. The diffraction lines are both indexed with an $R\bar{3}m$ space group in the rhombohedral system. The obvious separation of (0 0 6)/(1 0 2) and (1 0 8)/(1 1 0) doublets further indicates a favorable stacking order for layered cathode materials [28].

The compatibility of PEO_{20}–LiBOB and PEO_{20}–LiBOB–5 wt% MgO toward prepared $LiCoO_2$ and $LiNi_{1/3}Co_{1/3}Mn_{1/3}O_2$ is studied. The charge and discharge curves for the Li|PEO_{20}–LiBOB|$LiNi_{1/3}Co_{1/3}Mn_{1/3}O_2$ half cell in the initial, the third and the 20th cycles are shown in Fig. 4a. The characteristic voltage plateau for $LiNi_{1/3}Co_{1/3}Mn_{1/3}O_2$, at 3.75 V, is clearly visible. The charge capacity and discharge capacity are 168.8 and 156.8 mAh g^{-1}, respectively, in the first cycle at a 0.2*C*-rate,

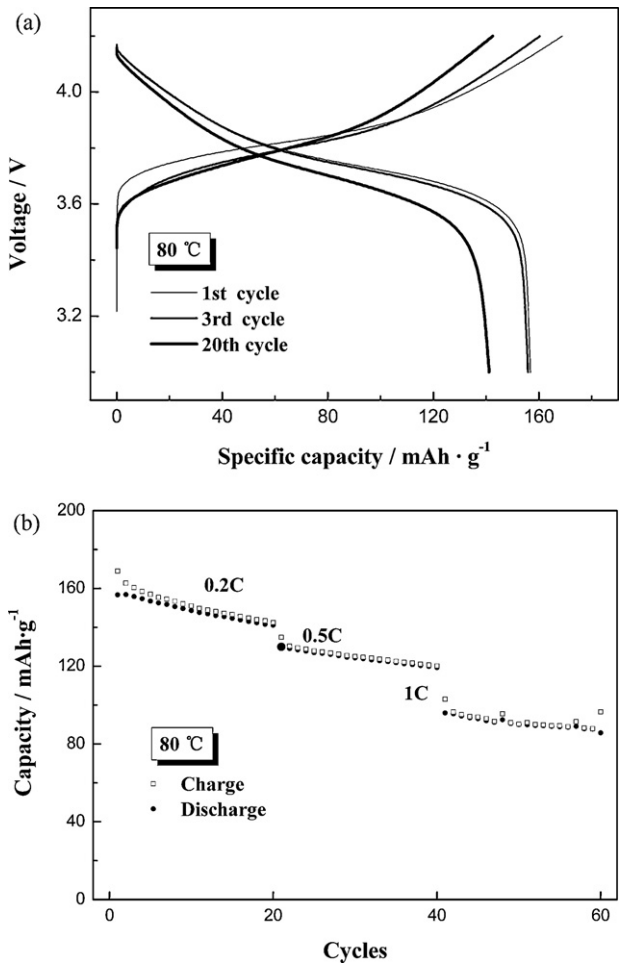

Fig. 5. Charge and discharge curves of the first, third and twentieth cycle at 0.2*C*-rate (a) and the cycling performance at 0.2*C*-rate, 0.5*C*-rate and 1*C*-rate (b) for the Li|PEO_{20}–LiBOB|LNCMO cell between 3.0 and 4.2 V at 80 °C.

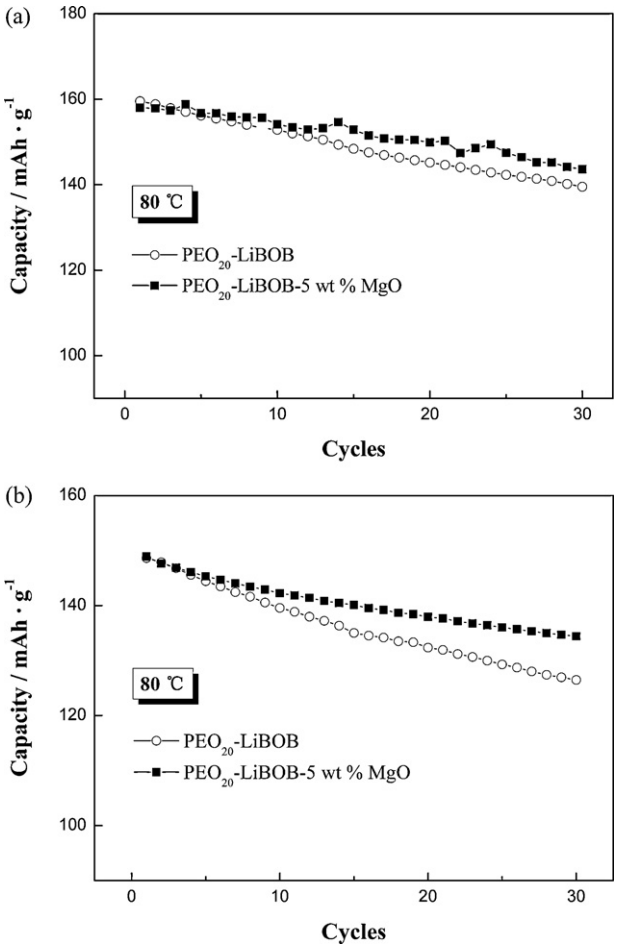

Fig. 6. Comparison of discharge profiles between Li|PEO_{20}–LiBOB–5 wt% MgO|$LiNi_{1/3}Co_{1/3}Mn_{1/3}O_2$ cell and Li|PEO_{20}–LiBOB|$LiNi_{1/3}Co_{1/3}Mn_{1/3}O_2$ cell (a), as well as between Li|PEO_{20}–LiBOB–5 wt% MgO|$LiCoO_2$ cell and Li|PEO_{20}–LiBOB|$LiCoO_2$ cell (b), at 0.2*C*-rate between 3.0 and 4.2 V at 80 °C.

being 30 mA g^{-1} in current density. The irreversible capacity is 12.0 mAh g^{-1}, and the initial coulomb efficiency is 92.9%.

The discharge capacity merely changes in the first three circles, but gradually degrades to 142.5 mAh g^{-1} after 20 cycles. The decreasing rate is 0.7 mAh g^{-1} per cycle, with retention of 90.9% discharge capacity. The cells present an interesting property that the coulomb efficiency increases to around 99.0% after several cycles. The charge and discharge processes are using the same current density during power capacity measurement, and corresponding results are summarized in Fig. 4b. Out of the relatively large capacity delivered at 0.2*C*-rate, the battery is still able to operate at 1*C*-rate. However, at 1*C*-rate the cells only deliver a capacity of about 95 mAh g^{-1}.

As to the nano-sized MgO enhanced SPE, PEO_{20}–LiBOB–5 wt% MgO, improved cycling performances are observed both for $LiCoO_2$ and $LiNi_{1/3}Co_{1/3}Mn_{1/3}O_2$ cells (Fig. 6). The comparisons of cycling performances are shown in Fig. 5a and b. The initial discharge capacity of PEO_{20}–LiBOB–5 wt% MgO cells, using $LiNi_{1/3}Co_{1/3}Mn_{1/3}O_2$ as the cathode, is almost identical to that of PEO_{20}–LiBOB cells at around 157 mAh g^{-1}. However, irreversible capacity is significantly decreased from 0.7 mAh g^{-1} to 0.5 mAh g^{-1} per cycle in 30 cycles at 0.2*C*-rate. When PEO_{20}–LiBOB is adopted as the electrolyte, $LiCoO_2$ possesses an initial discharge capacity of 148 mAh g^{-1}, which degrades to 124 mAh g^{-1} after 30 cycles at 0.2*C*-rate. The decreasing rate is 0.8 mAh g^{-1} per cycle, similar to that of $LiNi_{1/3}Co_{1/3}Mn_{1/3}O_2$. Comparatively, when PEO_{20}–LiBOB–5 wt% MgO is used as the electrolyte, the initial discharge capacity has little change but the irreversible capacity is decreased to 0.4 mAh g^{-1} per cycle.

The good compatibility of LiBOB containing PEO-based SPEs, towards 4 V class cathodes, is due to lithium salt LiBOB. Abundant carbonyl group in BOB^- anion could possibly play a critical role to passivate the cathode via a ring-opening reaction to generate a linear inorganic lithium metaborate film that covers the cathode surface. The passivation of the cathode surface by oxidization product of electrolyte component, mainly LiBOB here, will prevent further oxidization and thus reduce side reaction. Therefore, kinetic stability is obtained for real cathodes material, favoring reversible electrode reaction occurring in the cathode surface. On the other side, such promising stability of LiBOB-adopted SPE also can be partly due to the reaction property of LiBOB towards water. Water is currently difficult to be completely avoided during the preparation of SPEs, as well as the fabrication process and working condition for cells. Hydrolysis of LiBOB has been proved to have little effect on cycling performance of cathodes, for it decomposes into less corrosive compounds both at ambient temperature and at moderate temperature in the presence of moisture [29]. Adoption of nano-sized metal oxide such as MgO further eliminates the effect of water and unstable compounds involved in side reactions, leading to higher anodic stability and reduced interface impedance between electrolyte and lithium metal anode and thus improved cycling performance are observed for the cells using PEO_{20}–LiBOB–5 wt% MgO as the electrolyte.

4. Conclusion

Addition of nano-sized metal oxide MgO to PEO_{20}–LiBOB can enhance the intrinsic anodic stability and decrease the electrolyte|lithium–metal–anode interface impedance. Due to the property of LiBOB, remarkable kinetic stability is obtained for the SPEs within the voltage ranges of 3.0–4.5 V. The kinetic stability efficiently supports the cycling of 4 V class cathodes materials $LiNi_{1/3}Co_{1/3}Mn_{1/3}O_2$ and $LiCoO_2$. The former shows an initial capacity of 156.8 mAh g^{-1}, with retention of 142.5 mAh g^{-1} after 20 cycles at 0.2*C*-rate. The cell exhibits good cycling performance up to 1*C*-rate. Meanwhile, nano-MgO enhanced SPE presents even better performance towards real cathodes. The irreversible capacity per cycle has been successfully reduced by using PEO_{20}–LiBOB–5 wt% MgO as the electrolyte. Finally, we state that lithium salt anion plays an important role in determining the actual performance for polymer electrolytes. The application of LiBOB and nano-sized metal oxides may be a convenient and economic way to develop PEO based polymer electrolytes for 4 V class cathodes.

Acknowledgement

This work was supported by National High Technology Research and Development Program of China under Grant No. 2008AA11A102.

References

[1] D. Aurbach, A. Zaban, A. Schechter, Y. Ein-Eli, E. Zinigrad, B. Markovsky, Journal of the Electrochemical Society 142 (1995) 2873–2882.
[2] K. Xu, Chemical Reviews 104 (2004) 4303–4417.
[3] J.J. Auborn, Y.L. Barberio, Journal of the Electrochemical Society 134 (1987) 638–641.
[4] B. Scrosati, Journal of the Electrochemical Society 139 (1992) 2776–2781.
[5] K. Hayashi, Y. Nemoto, S.-i. Tobishima, J.-i. Yamaki, Electrochimica Acta 44 (1999) 2337–2343.
[6] F. Croce, G.B. Appetecchi, L. Persi, B. Scrosati, Nature 394 (1998) 456–458.
[7] F. Gray, M. Armand, in: J.O. Besenhard (Ed.), Handbook of Battery Materials, Wiley-VCH, Weinheim, 1999, p. 499.
[8] F. Croce, R. Curini, A. Martinelli, L. Persi, F. Persi, F. Ronsi, B. Scrosati, Journal of Physical Chemistry B 103 (1999) 10632–10638.
[9] J. Xi, X. Qiu, M. Cui, X. Tang, W. Zhu, L. Chen, Journal of Power Sources 156 (2006) 581–588.
[10] M. Morita, H. Noborio, N. Yoshimoto, M. Ishikawa, Solid State Ionics 177 (2006) 715–720.
[11] B. Scrosati, F. Croce, S. Panero, Journal of Power Sources 100 (2001) 93–100.
[12] H. Sumathipala, J. Hassoun, S. Panero, B. Scrosati, Ionics 13 (2007) 281–286.
[13] F. Croce, L. Settimi, B. Scrosati, Electrochemistry Communications 8 (2006) 364–368.
[14] Y. Aihara, J. Kuratomi, T. Bando, T. Iguchi, H. Yoshida, T. Ono, K. Kuwana, Journal of Power Sources 114 (2003) 96–104.
[15] S. Seki, S.-i. Tabata, S. Matsui, M. Watanabe, Electrochimica Acta 50 (2004) 379–383.
[16] D. Aurbach, Journal of Power Sources 89 (2000) 206–218.
[17] K. Edström, T. Gustafsson, J.O. Thomas, Electrochimica Acta 50 (2004) 397–403.
[18] W. Xu, C.A. Angell, Electrochemical and Solid-State Letters 4 (2001) E1–E4.
[19] K. Xu, S. Zhang, T.R. Jow, W. Xu, C.A. Angell, Electrochemical and Solid-State Letters 5 (2002) A26–A29.
[20] K. Xu, S.S. Zhang, B.A. Poese, T.R. Jow, Electrochemical and Solid-State Letters 5 (2002) A259–A262.
[21] U. Lischka, U. Wietelmann, M. Wegner, German Pat. DE 19829030 (1999) C1.
[22] G.B. Appetecchi, D. Zane, B. Scrosati, Journal of the Electrochemical Society 151 (2004) A1369–A1374.
[23] Y. Huang, J. Chen, J. Ni, H. Zhou, X. Zhang, Journal of Power Sources 188 (2009) 538–545.
[24] M. Handa, M. Suzuki, J. Suzuki, H. Kanematsu, Y. Sasaki, Electrochemical and Solid-State Letters 2 (1999) 60–62.
[25] O. Chusid, Y. Gofer, D. Aurbach, M. Watanabe, T. Momma, T. Osaka, Journal of Power Sources 97–98 (2001) 632–636.
[26] D. Guyomard, J.M. Tarascon, Journal of the Electrochemical Society 140 (1993) 3071–3081.
[27] J.B. Goodenough, Y. Kim, Chemistry of Materials 22 (2009) 587–603.
[28] K.S. Park, M.H. Cho, S.J. Jin, K.S. Nahm, Electrochemical and Solid-State Letters 7 (2004) A239–A241.
[29] K. Xu, S.S. Zhang, U. Lee, J.L. Allen, T.R. Jow, Journal of Power Sources 146 (2005) 79–85.